Available online at www.sciencedirect.com
SCIENCE DIRECT®
Journal of Power Sources 136 (2004) 401–407
JOURNAL OF POWER SOURCES
www.elsevier.com/locate/jpowsour

Switch array system for thin film lithium microbatteries

Vinesh Sukumar [a,*], Mahmoud Alahmad [a], Kevin Buck [a], Herbert Hess [a], Harry Li [a], Dave Cox [a], Fadi Nessir Zghoul [a], Jeremy Jackson [b], Stephen Terry [b], Ben Blalock [b], M.M. Mojarradi [c], W.C. West [c], J.F. Whitacre [c]

[a] *Microelectronics Research and Communications Institute, University of Idaho, Moscow, ID, USA*
[b] *Integrated Circuits and Systems Laboratory,University of Tennessee, Knoxville, TN, USA*
[c] *Jet Propulsion Laboratory, California Institute of Technology, Pasadena, CA, USA*

Available online 2 June 2004

Abstract

Integrated microbatteries are currently being developed to provide reliable low-noise voltage sources for system-on-a-chip applications by Jet Propulsion Laboratory (JPL). These microbatteries help provide localized current capacities or embedded power supplies at the chip level for space exploration. This paper presents a design approach for charging and discharging microbatteries. Maximum flexibility in terms of voltages and currents are also obtained through the use of a switching matrix. The microbatteries used for the design are rated at 50 nAh capacity and are solid-state lithium electrolyte based. The designs are built using Microwave Silicon-on-Insulator process.

Keywords: LDMOSFET; Micropower; Microbattery; SOI

1. Introduction

NASA engineers have been working to develop a conceptual design for microspacecraft, which would have all important features and have a reduction in mass. NASA plans to achieve this by the miniaturization and integration of power sources with their loads [1]. This highly integrated approach would also be useful for analogous commercial, aerospace, and military applications. By providing point-of-use power, significant reduction in mass associated with wiring and packaging can be obtained. Similar advantages can be utilized by colocating micropower sources and integrated circuit components on the same chip.

Thin film lithium microbatteries have emerged as a legitimate power source in many microspacecraft applications. Conventional bandgap voltage reference circuits can be quite large, and are candidates for replacement by these microscale batteries. Analog sensors, which require total isolation from digital noise for optimal performance can benefit from these on-chip power sources [2].

The capacity and current rating of any microbattery is limited. Certain miniaturized systems require higher capacities and voltages than a single microbattery can provide. This paper describes a microbattery switch array system in Silicon-on-Insulator, which groups multiple lithium microbatteries to form a microbattery array. This approach provides maximum voltage and capacity flexibility at the chip level.

This switch matrix will also be useful in providing on-chip power for several low-current, high-voltage applications in microspacecraft systems.

2. Microbattery characteristics

The microbatteries used for the project have been designed, fabricated, and tested at JPL, California Institute of Technology [2]. The characteristics of the microbatteries are listed in Table 1. The lithium microbatteries fabricated for this work were nominally 600 μm × 600 μm, and provided between 10–50 nAh capacity (Fig. 1). These microbatteries can be cycled hundreds of times with minimal capacity loss (Fig. 2) [2].

3. Microbattery charging algorithms

After practicing several charging algorithms, a constant current constant voltage (CCCV) method was found to be

* Corresponding author. Tel.: +1-208-885-4341.
E-mail address: vinesh@mrc.uidaho.edu (V. Sukumar).

0378-7753/$ – see front matter © 2004 Elsevier B.V. All rights reserved.
doi:10.1016/j.jpowsour.2004.03.033

Table 1
Characteristics of lithium microbattery

Lithium battery	Characteristics
Capacity	1–200 nA h
Voltage rating	
Rated voltage	4.25 V
Maximum overcharge voltage	4.3–4.4 V
Electrical breakdown	5.5 V
Operating range	4.25–3 V
Deep discharge to	0 V
Charge/discharge rating	
Rate of charge	0.1–10 C
Effecient rate	0.1–0.15 C
Normal rate	1.0 C

reliable and efficient. In this method a lithium microbattery is charged at a set current level (normally equal to 1 C (capacity) rating of the microbattery) until it reaches its final voltage. At this point, the charger circuitry switches over to constant voltage mode, and provides the current necessary to hold the microbattery at this final voltage (4.25 V/cell). During the constant voltage phase, current drops exponentially to a zero value. Thus, the charger should be capable of providing stable control loops for maintaining either current or voltage at a constant value, depending on the state of the microbattery [3]. To maximize useful charge cycle time, the CCCV was removed as soon as the charging current reached 5% of the constant current value. At this point it was observed that the microbattery capacity reached 95–99% of the rated value [3].

Table 1 indicates that the capacity of the microbatteries is in the nano-ampere–hour range. As such, it is challenging to generate a very accurate nano-ampere current source using discrete components. To overcome this difficulty, pulse charging is considered because these microbatteries responded well to pulses of current. It is our experience that the microbatteries can tolerate pulse charging without any apparent deleterious effects. The basic concept is to charge thin film microbatteries with large values of current, but with a small duty cycle at high frequencies. This produces a fairly accurate net lower average current.

In a microbattery stack array, it is advisable that the microbatteries be charged in parallel. Serial charging is not practiced because of the difficulty in maintaining voltage balance. This allows the charger circuitry to be simpler in design as well.

After several lab-based charge/discharge experimental trials involving lithium microbatteries using discrete components, it was concluded that the integrated charger could use either the CCCV method or the pulse-charge algorithm to charge the microbatteries and achieve acceptable results.

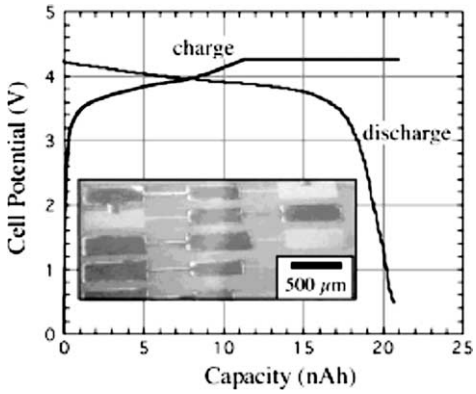

Fig. 1. Charge and discharge profile of a lithium microbattery.

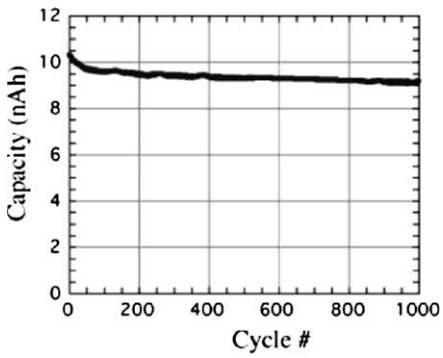

Fig. 2. Capacity behavior as a function of charge cycles.

4. Microbattery power management system

Fig. 3 is a block diagram representation of the integrated microbattery power management system (μBPMS), developed using Silicon-on-Insulator process rules. The μBPMS is a system designed for programmability and flexibility features for a microbattery cell. Such features include charge/discharge option, and characteristic monitoring of each cell. In addition, the system maintains a look-up table indicating such parameters as number of charged cells, number of cells to be charged, number of faulty cells, and the number of times a given cells has been charged/discharged. These data will be available to the user as a real-time status of the system. The charge mechanism can be applied to single cells or multi-cells connected in

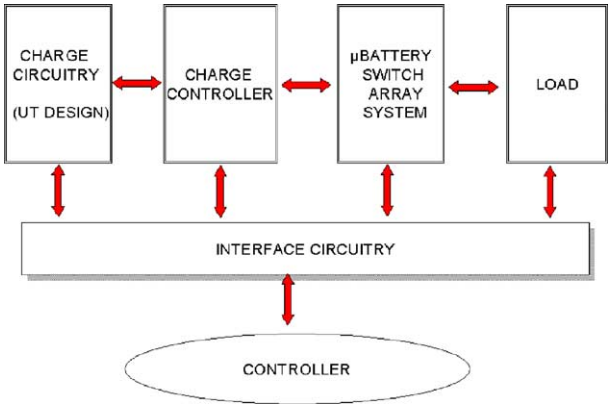

Fig. 3. Microbattery power management system level architecture.

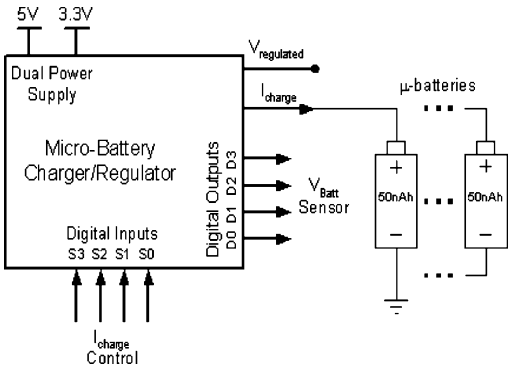

Fig. 4. Microbattery charger architecture.

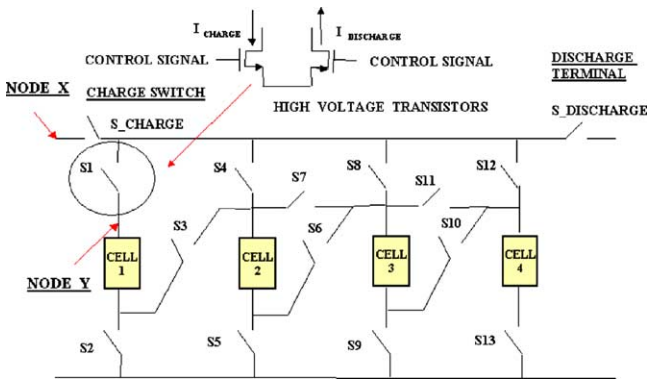

Fig. 5. Switch matrix for the microbattery switch array system.

parallel. The discharge mechanism can be applied to single cells or multi cells connected in parallel for user-defined capacity requirements or cells connected in series for user defined voltage values.

The μBPMS consists of five parts: charge circuitry, charge controller, μBPMS battery switch array system, interface circuitry, and controller as shown in Fig. 3. The charge circuitry is a system that provides fifteen different current values in increments of 50 nA and a constant voltage level. The current increments and/or constant voltage can be selected to charge the cells as required by the system. The charge controller system provides additional charge flexibility to the user by allowing pulse charging to be incorporated into the charging mechanism. The μBPMS consists of two parts: a switch matrix and switch matrix controller. The switch matrix allows the system to connect *N* cells in any desired configuration. While the switch matrix controller provides the desired control signals to achieve the desired configuration. The interface circuitry is a system component that allows the controller to communicate with the individual components of the μBPMS. The controller is a software/hardware integrated system that monitors the operation of the individual components of the system and performs tasks as outlined in the system specifications [4].

Fig. 4 is the block diagram representation of the University of Tennessee's charger circuitry. The charger provides a digitally adjustable output current in increments of 50 nA up to a maximum of 750 nA. The output current is controlled using a four-bit, current-mode digital-to-analog converter (DAC). The controller is responsible for sending the four-bit control word to the charger circuitry. The constant voltage charging capability of 4.25 V is implemented using a voltage regulator circuit. A flash analog-to-digital converter (ADC) constantly monitors the microbattery voltage and signals the charge controller when the microbattery is at full voltage capacity.

5. Microbattery switch matrix design issues

The microbattery switch matrix helps in providing the maximum voltage and current capacities that approach theoretical values. As seen in Fig. 5, for charging cell 1, switches S1, S2, and S_CHARGE are fully on with the other terminal switches being fully off. The same principle applies for charging other cells individually with the appropriate switches turned on.

For discharging cell 1, switches S1, S2, and S_DISCHARGE are fully on to form the closed loop circuit. The switch matrix also helps achieve series discharge. As seen in the schematic, if there exists a series discharge path with all cells connected in series, then node Y experiences a potential of 17 V (4×4.25 V). It is an important design issue that the switches handle such a high value of voltage without experiencing electrical breakdown. At the same time, it can be observed that the switch S1 is used for both charging and discharging cell 1. As such, the switch must be bi-directional. It is desirable that the forward voltage drop associated with each switch during charging a cell be as small as possible. If one desires to retain a fully charged microbattery, for example, cell 1, then switch S1 has to be fully off with no leakage present. If switch S1 experiences leakage, then there exists a possibility wherein cell 1 could lose charge to Node X through switch S1. Initially, high voltage diodes were used for the design of the switches, but experimental results showed that the leakage were in the range of 17 nA and, as such the design was discarded. After several experimental trials, high voltage metal oxide semiconductor (MOS) switches were found that satisfy the leakage requirements. A separate array of switches are used for charging and discharging the cells, as explained in the next section of the paper.

6. Different working cases of a switch matrix for the microbattery switch array system

Using the switch matrix in Fig. 5, four possible operating cases can be envisioned to charge and discharge microbatteries.

6.1. Charging any individual microbattery

In any given microbattery stack array, there exists a possibility wherein a single microbattery requires charge. Such

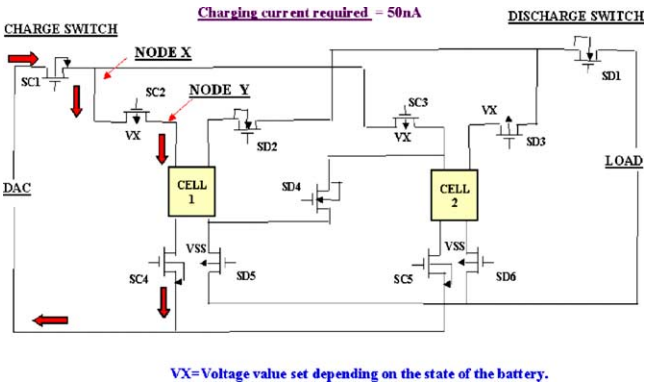

Fig. 6. Charging any single microbattery.

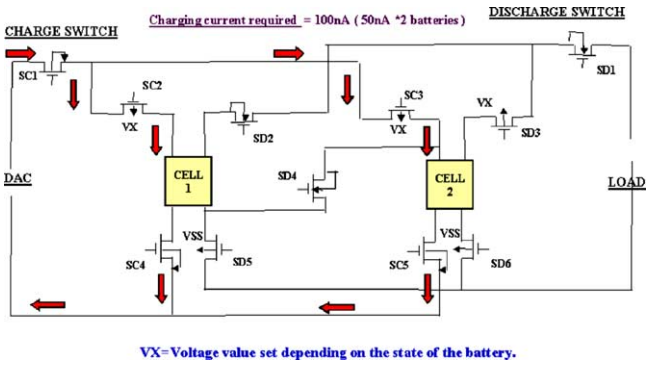

Fig. 7. Charging microbatteries in parallel.

microbatteries would require charging current for a fully charged condition. Fig. 6 schematic shows one method to achieve this. The charging current is limited to a 1-C rating of the microbattery, which is equivalent to 50 nA of current. The gate voltages for each of the MOS switches is provided by a gate driver controller.

At any point of charge cycle time, it is important that the voltage of the microbattery be known. This is because the microbattery voltage sets the gate voltage of the charging switch. For example, if the microbattery voltage is at 4.10 V, then the microbattery requires charging current to reach end-of-charge threshold value of 4.25 V. If the gate voltage of switch SC2 is kept at 5 V, then the device SC2 is not in a strong inversion region. This tends to limit the amount of charging current going into cell 1. This is overcome by increasing the gate voltage to a higher value, e.g. 6 V. Now, if the same gate voltage is maintained and if the microbattery voltage is at 0 V, this could lead to device gate oxide breakdown.

Switch SC2 has an isolated bulk. This is because, when cells 1 and 2 are connected in series, the positive side of cell 1 is raised to a potential of 8.50 V (2×4.25 V). This forward biases the internal pn diode formed between the source and bulk, yielding a flow of current from node X to node Y, which is an undesirable factor. This has been eliminated by isolating the bulk and reverse biasing the pn diode.

6.2. Charging microbatteries in parallel

It is always advisable that all the microbatteries in a stack array be charged at the same time so that they obtain equal microbattery voltages. The microbatteries can be charged both serially and in parallel. Series charging is not practical because it is difficult to balance the microbattery voltages. Parallel charging offers the advantage of microbatteries automatically reaching an equivalent potential value. Fig. 7 depicts how microbatteries can be charged in parallel. Switch SC3 has an isolated bulk and holds the same explanation as switch SC2.

6.3. Discharging microbatteries in parallel

The microbattery switch matrix also assists in providing increased current capacities to the load. This is achieved by discharging microbatteries in parallel. Since each of these microbatteries are rated at 50 nAh, it is possible to provide 100 nA of current for 1 h to the load before the microbatteries reach the lower end-of-charge threshold voltage. P-channel MOS devices are used as switches during the discharge as seen in Fig. 8. The gate voltages of the P-channel MOS devices (SD2 and SD1) are pulled low. This forces the device to operate in a strong inversion region. As such, maximum energy can be harnessed from the microbatteries. Higher current capacities can be obtained by increasing the number of microbatteries in the switch matrix.

6.4. Discharging microbatteries in series

The microbattery switch matrix also facilitates in providing increased supply voltages (Fig. 9) at the chip level and thereby eliminating area used by power supply circuits. Ideally speaking, since each of these microbatteries has a full-scale voltage reading of 4.25 V, it is again possible to provide 8.50 V for a period of 1 h before the microbatteries reach their threshold voltage value. The gate voltage for switch SD2 is maintained at 5 V [5]. This is done so that the switch exhibits an automatic disconnect behavior when the combined cell voltage reaches 6 V. This limits the

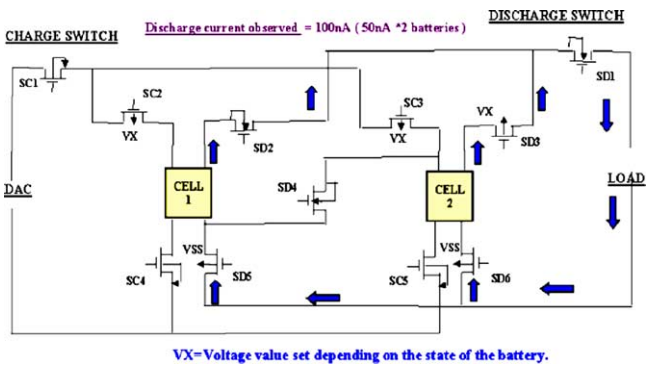

Fig. 8. Discharging microbatteries in parallel.

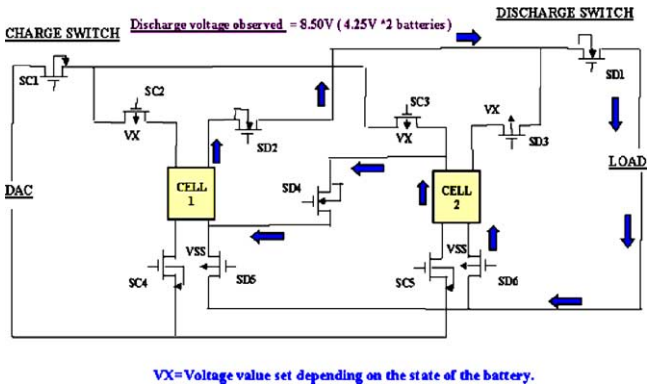

Fig. 9. Discharging microbatteries in series.

microbattery voltage to 3 V/cell assuming that we have identical microbatteries. To avoid capacity degradation, overcharge or deep discharge is not practiced.

7. Computer simulation results

Simulation results of the switch matrix using 3.3 V Silicon-on-Insulator SPICE models at room temperature are shown in Figs. 11–14. Fig. 11 shows the simulated voltage behavior of the switch matrix controller for charging two microbatteries in parallel.

A parallel RC model (Fig. 10) for a microbattery is assumed during the simulation trials. A current of 100 nA was used to charge two identical RC networks [6]. The value of the resistor in the RC model was chosen as shown below.

$$\mathrm{RA} = \frac{4.25\,\mathrm{V}}{50\,\mathrm{nA}} = 85\,\mathrm{Meg} \quad (1)$$

The 4.25 V in Eq. (1) is the rated full-scale rated voltage of the microbattery and 50 nA is equivalent to 1 C rating of the microbattery. The time constant (τ) was maintained at around 520 s [7]. This led to a capacitance of approximately 6 μF as shown below

$$\mathrm{CA} = \frac{\tau}{R} = \frac{520\,\mathrm{s}}{85\,\mathrm{Meg}} = 5.88\,\mu\mathrm{F} \quad (2)$$

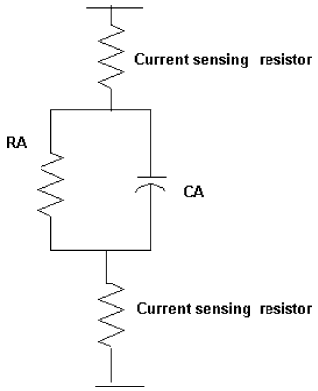

Fig. 10. RC model used for the microbattery.

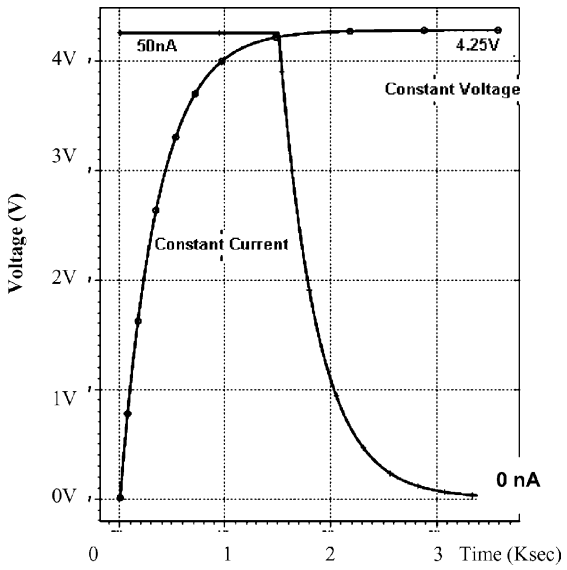

Fig. 11. Charging microbatteries in parallel.

This model only accounts for the microbattery capacity and does not necessarily predict realistic current–voltage profiles as a function of time.

The constant current behavior and the constant voltage behavior are as shown in Fig. 11. A total of 5 pA of leakage currents was observed during simulations as seen in Fig. 14. The maximum gate source voltage at any given point of time during charging was limited to 6 V.

Fig. 12, another simulation example, shows how the microbatteries can be discharged in parallel to produce increased current capacities. A resistive load is presumed at the output terminals. Again, it is assumed that the microbatteries have identical ratings. In this mode, switch SD1 shows a forward voltage of 18 mV due to increased current

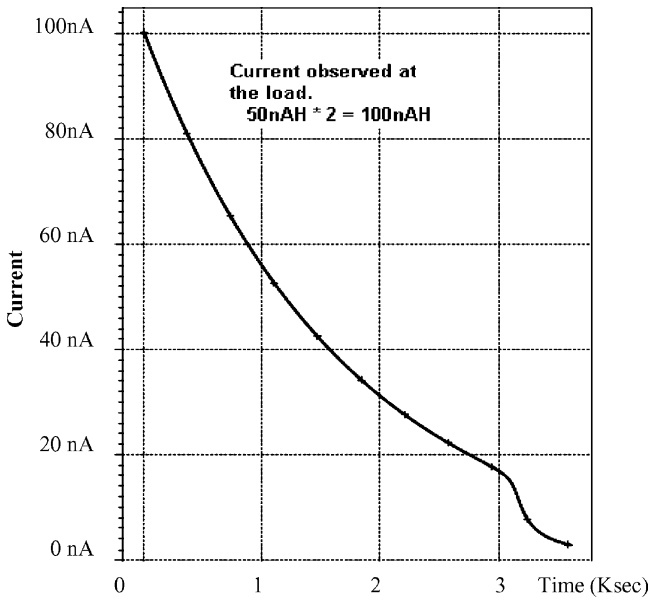

Fig. 12. Discharging microbatteries in parallel.

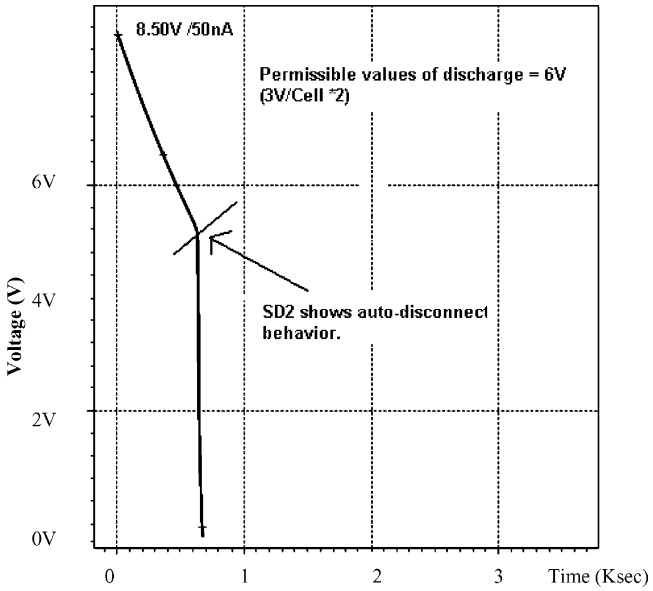

Fig. 13. Leakage current measurements.

flow. The other conducting switches maintain a drop of 10 mV.

Fig. 13 shows how the microbatteries discharge in series mode, with automatic self-disconnect configuration. The series grouping allows microbatteries to achieve higher voltage value of 8.50 V. The microbatteries are allowed to discharge to a combined value of 6 V, before the discharge switch turns itself off.

Fig. 14 shows the amount of leakage associated with the MOS switches. In this simulation, a fully charged microbattery was assumed with appropriate gate voltages applied to the switches so that they are in the off state [8]. A resistive load of 85 Meg with a pad capacitance of 20 pF was assumed for the simulations. An output voltage of 430 μV was observed at the load under blocking conditions inferring a leakage current of 5 pA. This simulation points out that isolation could be achieved with little to no energy loss from the microbattery. Also, the forward voltage for any conducting MOS switch was observed to be close to 10 mV.

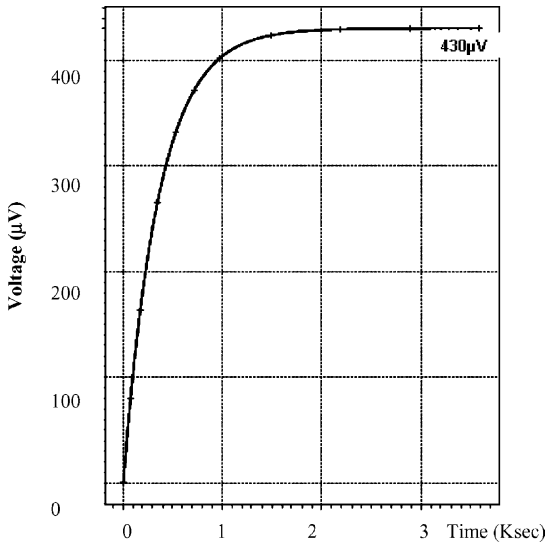

Fig. 14. Leakage current measurements.

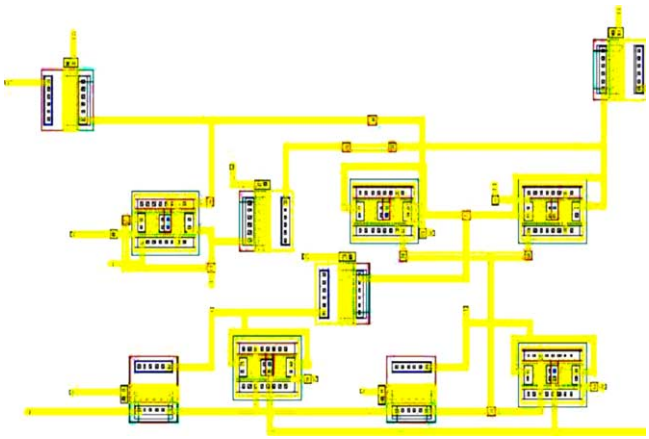

Fig. 15. Map of layout for microbattery switch matrix.

A gate/bulk driver circuit for the microbattery switch matrix has been developed that will be addressed in a future paper [8]. It drives the switches in a reliable manner. From the above-based simulations, it is safe to conclude that the microbattery switch matrix will perform as desired.

The discharge profiles do not necessarily replicate ideal microbattery discharge characteristics. The simulations are used to prove that the switch matrix allows energy transfer to the load without any loss of energy.

8. Test chip

A test chip is being fabricated in a 0.35-μm Silicon-on-Insulator process as seen in Fig. 15. Upon completion of fabrication, its performance will be appropriately reported.

9. Conclusions

A switch matrix for two microbatteries is successfully developed. The designed switch matrix is a subset of a complete microbattery power management system. The two-cell microbattery switch matrix is an implementation of the general microbattery switch array system discussed earlier. It helps in charging two microbatteries in parallel and at the same time also allows two microbatteries to be discharged in series or parallel mode. Using a simple model of the microbattery in the SPICE simulations, MOS devices show negligible device leakage (<5 pA) and also less than 10 mV forward drop on any switch. This is appropriate for any microbattery charge of the stated size (50 nAh microbattery).

Acknowledgements

The work described in this paper was carried out for the JPL, California Institute of Technology, under a contract with the NASA.

References

[1] W.C. West, J.F. Whitacre, E.J. Brandon, B.V. Ratnakumar, Fabrication and testing of all solid-state microscale lithium batteries for microspacecraft applications, J. Micromech. Microeng. 12 (1) (2002) 58–62.
[2] W.C. West, J.F. Whitacre, E.J. Brandon, B. V Ratnakumar, Lithium micro-battery development at the jet propulsion laboratory, IEEE AESS Sys. Mag. 16 (8) (2001) 31–33.
[3] D. Linden, T. B. Reddy, Handbook of Batteries, 3rd ed., 1998.
[4] A. Davis, S.S. Eaves, Z.M. Salemeh, Evaluation of lithium ion synergetic battery pack as a battery charger, IEEE Trans. Energy Conv. 14 (3) (1999) 830–835.
[5] M. Alahmad, V. Sukumar, H. Hess, K.M. Buck, H. Li, D. Cox, Behavior and Characteristics Analysis of a Rechargeable Micro-Scale Lithium Battery for an Intelligent Power Management System, to be presented at the 205th Meeting of the Electrochemical Society, May 9–14, 2004.
[6] S.C. Hageman, Simple PSPICE Models Let You Simulate Complex Battery Types. EDN, Oct. 1993, pp. 117–132.
[7] V. Sukumar, H. Hess, H. Li, D. Cox, M. Alahmad, F.N. Zougl, K. Buck, Nano Current Charging Algorithm For Thin Film Lithium Ion Microbatteries, 11th NASA Symposium On The VLSI Design, Coeur d'Alene, Idaho, 28–29 May 2003.
[8] V. Sukumar, Design of a MOSFET Driven Switch Array System for Lithium Microscale Batteries in Microwave Silicon-on-Insulator (MOI5) 0.35 μm Process for Aerospace Applications, MS Thesis, University of Idaho, August 2003.